Role of MHC-Linked Genes in Autoantigen Selection and Renal Disease in a Murine Model of Systemic Lupus Erythematosus[1]

Hideharu Sekine,[2]* Kareem L. Graham,[†] Shenru Zhao,[†] Margaret K. Elliott,* Philip Ruiz,[‡] Paul J. Utz,[†] and Gary S. Gilkeson*

We previously described a renal protective effect of factor B deficiency in MRL/*lpr* mice. Factor B is in the MHC cluster; thus, the deficient mice were $H2^b$, the haplotype on which the knockout was derived, whereas the wild-type littermates were $H2^k$, the H2 of MRL/*lpr* mice. To determine which protective effects were due to H2 vs factor B deficiency, we derived $H2^b$ congenic MRL/*lpr* mice from the 129/Sv ($H2^b$) strain. Autoantibody profiling using autoantigen microarrays revealed that serum anti-Smith and anti-small nuclear ribonucleoprotein complex autoantibodies, while present in the majority of $H2^{k/k}$ MRL/*lpr* mice, were absent in the $H2^{b/b}$ MRL/*lpr* mice. Surprisingly, 70% of MRL/*lpr* $H2^{b/b}$ mice were found to be serum IgG3 deficient (with few to no IgG3-producing B cells). In addition, $H2^{b/b}$ IgG3-deficient MRL/*lpr* mice had significantly less proteinuria, decreased glomerular immune complex deposition, and absence of glomerular subepithelial deposits compared with MRL/*lpr* mice of any H2 type with detectable serum IgG3. Despite these differences, total histopathologic renal scores and survival were similar among the groups. These results indicate that genes encoded within or closely linked to the MHC region regulate autoantigen selection and isotype switching to IgG3 but have minimal effect on end-organ damage or survival in MRL/*lpr* mice. ***The Journal of Immunology,*** **2006, 177: 7423–7434.**

Major histocompatibility complex haplotypes encode scores of immunologically important genes, including the highly polymorphic MHC class I and class II gene clusters, complement cascade components (*C4*, *C2*, and *factor B*), cytokines (*Tnfa* and *Lta*), proteins involved in Ag processing (*Lmp2* and *Tap1*), and chaperones (*Hsp70*) (1, 2). The murine H2 region, located on chromosome 17, is orthologous with the human MHC on chromosome 6. An exception is the class I region in which the composition and arrangement of class Ib genes differ markedly. MHC haplotypes are genetic determinants of susceptibility to multiple diseases with an autoimmune etiology, including type 1 diabetes, multiple sclerosis, rheumatoid arthritis, and systemic lupus erythematosus (SLE)[3] (3, 4).

SLE is a prototypic autoimmune disease characterized by production of autoantibodies, as well as inflammation in target organs, including the kidneys (5). A host of autoantigens are targeted in humans and in murine models of SLE, including components of the nucleosome (e.g., histones and DNA), the U1-small nuclear ribonucleoprotein complex (U1-snRNP), the Ro/La complex, and phospholipids. Genome-wide scans of SLE multiplex families revealed that MHC is the strongest of candidate lupus susceptibility loci. Using a variety of MHC gene markers, population-based studies showed that the MHC class II DR-*B1* alleles DR2 and DR3 are associated with SLE in European-Caucasian populations (6, 7). However, MHC gene associations with SLE are complicated by the existence of extended HLA haplotypes in which class II genes are in significant linkage disequilibrium with other potential lupus susceptibility genes, including *C4*, *C2*, *Tnfa*, and other MHC class III genes, (6).

New Zealand Black (NZB)/New Zealand White (NZW), BXSB, and MRL/*lpr* are inbred mouse strains that spontaneously develop a disease similar to human SLE (8). The genetic basis of disease in lupus-prone mice is complex. However, data from backcross and intercross experiments demonstrated linkage of disease with genes encoded within or closely linked to the MHC locus in NZB/NZW and BXSB mice (9). However, similar studies in MRL/*lpr* mice have not established a link between MHC and disease expression (10). Class II expression appears required for disease in MRL/*lpr* mice because MHC class II-deficient MRL/*lpr* mice ($H2^b$) did not produce serum anti-DNA Abs or develop proliferative renal disease in contrast to their wild-type ($H2^k$) counterparts (11). However, a direct link between these findings and MHC class II-deficiency is still

*Department of Medicine, Division of Rheumatology and Immunology, Medical University of South Carolina and the Medical Research Service, Ralph H. Johnson Veterans Affairs Medical Center, Charleston, SC 29425; †Department of Medicine, Division of Immunology and Rheumatology, Stanford University School of Medicine, Stanford, CA 94305; and ‡Department of Pathology, University of Miami School of Medicine, Miami, FL 33125

Received for publication April 24, 2006. Accepted for publication August 24, 2006.

The costs of publication of this article were defrayed in part by the payment of page charges. This article must therefore be hereby marked *advertisement* in accordance with 18 U.S.C. Section 1734 solely to indicate this fact.

[1] This work was supported by the Medical Research Service, Ralph H. Johnson Veterans Affairs Medical Center and National Institutes of Health Grant AI47469. K.L.G. was supported by a National Institutes of Health National Research Service Award Fellowship AI10663. P.J.U. was supported by the Northern California Chapter of the Arthritis Foundation, the Dana Foundation, the Stanford Program in Molecular and Genetic Medicine, National Institutes of Health Grants DK61934, AI50864, AI01514, and AR49328, National Heart, Lung, and Blood Institute Proteomics Contract N01-HV-28183, an Arthritis Foundation Arthritis Investigator Award, and a Baxter Foundation Award.

[2] Address correspondence and reprint requests to Dr. Hideharu Sekine, 96 Jonathon Lucas Street, Suite 912, P.O. Box 250637, Charleston, SC 29425. E-mail address: sekineh@musc.edu

[3] Abbreviations used in this paper: SLE, systemic lupus erythematosus; snRNP, small nuclear ribonucleoprotein complex; NZB, New Zealand Black; NZW, New Zealand White; RF, rheumatoid factor; Sm, Smith; DFU, digital fluorescence unit; SAM, significance analysis of microarray; GA, glomerular Ag; TMB, 3,3′,5,5′-tetramethylbenzidine; BBS, borate-buffered saline; EM, electron microscopy; GBM, glomerular basement membrane.

0022-1767/06/$02.00

unclear because the extended H2 of the MHC class II-deficient $H2^b$ mice was different from the control $H2^k$ MRL/*lpr* mice.

Lupus nephritis is a major cause of morbidity and mortality in human SLE, as well as in murine models of disease (12, 13). Deposition of glomerular immune complexes is the initiator of the inflammatory process in lupus nephritis (14, 15). Anti-DNA Abs are the predominant autoantibody eluted from glomeruli both in human SLE and MRL/*lpr* mice (16, 17). IgG3 is the dominant IgG isotype eluted from the kidneys of MRL/*lpr* mice (18), and IgG3 cryoglobulins with rheumatoid factor (RF) activity are associated with renal disease in this murine model (19, 20). We previously reported that MRL/*lpr* mice deficient in the alternative complement pathway component factor B develop less renal disease, survive longer, and a majority were serum IgG3 deficient. As the gene for factor B is in the MHC locus, the H2 of the factor B-deficient MRL/*lpr* mice was $H2^b$, the genotype of the strain (129/Sv) on which the factor B knockout was derived originally. The wild-type littermates were the H2 of MRL/*lpr* mice, $H2^k$. To determine which of the observed differences in factor B-deficient MRL/*lpr* mice were due to H2 vs factor B deficiency, we derived $H2^b$ MRL/*lpr* mice.

By comparing $H2^{k/k}$ wild-type MRL/*lpr* mice with the $H2^{b/b}$ congenic MRL/*lpr* mice, we provide evidence that genes within or closely linked to MHC are critical for specific features of disease. Protein microarray analysis demonstrated that $H2^{b/b}$ MRL/*lpr* mice lacked autoantibodies directed against Smith (Sm) and other snRNP autoantigens. The majority of MRL/*lpr* $H2^{b/b}$ mice was IgG3-deficient with decreased glomerular immune complex deposition, basement membrane subepithelial immune complex deposits, and proteinuria. These profound differences in phenotype, however, had no impact on proliferative renal disease, vasculitis, or survival.

Materials and Methods

Mice

129X1/SvJ (129/Sv; $H2^b$), C57BL/6J (B6; $H2^b$), BALB/cJ (BALB/c; $H2^d$), and MRL/MpJ-*Tnfrsf6lpr* (MRL/*lpr*; $H2^k$) mice were purchased from The Jackson Laboratory. Congenic MRL/*lpr* mice were developed for $H2^b$ or $H2^d$ by mating MRL/*lpr* mice with 129/Sv or B6 mice for $H2^b$ or BALB/c mice for $H2^d$ and backcrossing to MRL/*lpr* mice for three generations. After three generations of backcrossing, progeny were intercrossed to derive F_3 $H2^{b/b}$, $H2^{b/k}$, $H2^{d/d}$, $H2^{d/k}$, and $H2^{k/k}$ mice. 129/Sv-derived $H2^b$ MRL/*lpr* mice were further backcrossed for nine generations to derive F_9 $H2^{b/b}$, $H2^{b/k}$, and $H2^{k/k}$ MRL/*lpr* mice. At each generation, the haplotype of H2 was determined with four microsatellite markers (*D17Mit16* (centromeric of MHC), *H2 I-A* (MHC class II), *Tnfa* (MHC class III), and *D17Mit177* (telomeric of MHC)) that cover the entire MHC region. For F_9 mice, 136 polymorphic microsatellite markers (86 markers on chromosome 17; 50 markers on the other chromosomes) were screened for genotyping and verified that all of the markers outside of MHC region were MRL/*lpr*. Phenotypic confirmation of genetic markers was determined by flow cytometric analysis of H2 class I (K) and class II (I-A and I-E) expression on peripheral mononuclear cells. All F_9 congenic mice were confirmed homozygous for the *lpr* mutation in the Fas gene by PCR (21). Mice were bred and maintained under specific pathogen-free conditions at the animal facility of the Ralph H. Johnson Veterans Affairs Medical Center. The Ralph H. Johnson Veterans Affairs Institutional Animal Care and Use Committee approved the protocols used for experiments with mice.

Array production and probing

Screening of mouse serum for autoantibodies directed against major autoantigens in autoimmune rheumatic disease was performed using autoantigen microarray technology (22). A robotic arrayer was used to attach peptides and proteins to poly-L-lysine-coated slides (CEL Associates) in an ordered array (22, 23). Four to 12 replicate features of each peptide or protein were printed on each array. Spotted Ags included 36 recombinant or purified proteins, including Ro52, La, Jo-1, serine/arginine proteins, histones H1, H2A, H2B, and H3 plus H4, U1snRNP-BB′, U1–68 kD, U1snRNP-A, hnRNP-B1, Sm/RNP complex, Sm Ags, topoisomerase I, centromere protein B, and pyruvate dehydrogenase; 6 nucleic acid-based putative Ags, including dsDNA and ssDNA; and 154 overlapping synthetic peptides derived from snRNP proteins, Sm proteins, poly(ADP-ribose) polymerase, and histone H1, H2A, H3, and H4. Arrays were circumscribed with a hydrophobic marker, blocked overnight at 4°C in PBS containing 3% FCS and 0.05% Tween 20, incubated with 1/150 dilutions of mouse serum in blocking buffer for 1 h at 4°C, and washed twice in blocking buffer. Arrays were incubated with 1/4000 dilutions of cyanin 3 dye-conjugated goat anti-mouse IgG/M (Jackson ImmunoResearch Laboratories) for 1 h at 4°C and then washed twice in blocking buffer, PBS, and water. Arrays were spun dry and scanned with a Gene Pix 4000B scanner (Axon Instruments). Detailed protocols are published (22) and are available online (⟨www.stanford.edu/group/antigenarrays/⟩). False-color images derived from the scanned digital images are presented.

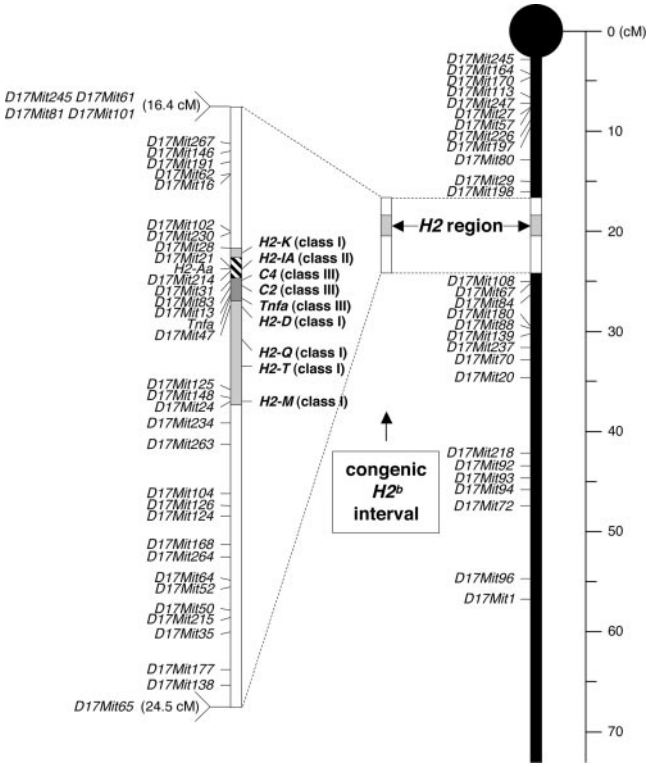

FIGURE 1. Detailed map of the 129/Sv interval in the F_9 $H2^b$ MRL/*lpr* mice on chromosome 17. The schema of mouse chromosome 17 (*right figure*) with the genetical scale is shown with the actual scale of the 129/Sv interval (*middle figure*). The enlarged 129/Sv interval is shown with H2 class I, II, and III genes (*left figure*). The 129/Sv interval, including the entire MHC loci ($H2^b$), spanned from ~16.4 to ~24.5 cM on chromosome 17. The microsatellite markers and gene polymorphisms used to characterize the introgressed 129/Sv region are shown at the *left side* of the figures.

Analysis of array data

The median feature and background pixel intensities for each Ag feature were determined using GenePix Pro 3.0 software (Axon Instruments), from which the net fluorescence intensity (expressed as digital fluorescence units (DFU)) was calculated for individual features. For each Ag, a raw value was generated from the median of net fluorescence values for all features representing that Ag (4–12 features per Ag). For statistical analysis, an adjustment of raw values was performed to eliminate negative values. If the raw value for an Ag was <1.0 on any array in the data set, the values for that Ag were adjusted for all arrays in the data set as follows: 1.0 plus the absolute value of the lowest raw value was added to the raw value for that Ag for all arrays in the data set to generate adjusted raw values. Normalization between arrays was then performed. For each array, the median of raw values for eight identical anti-mouse IgG features was used to normalize data sets between arrays. Adjusted raw values for each array were multiplied by a normalization factor so that the normalized median for the anti-mouse IgG reactivity was equal to 17,500. Normalized values were analyzed using the significance analysis of microarrays (SAM) algorithm (24).

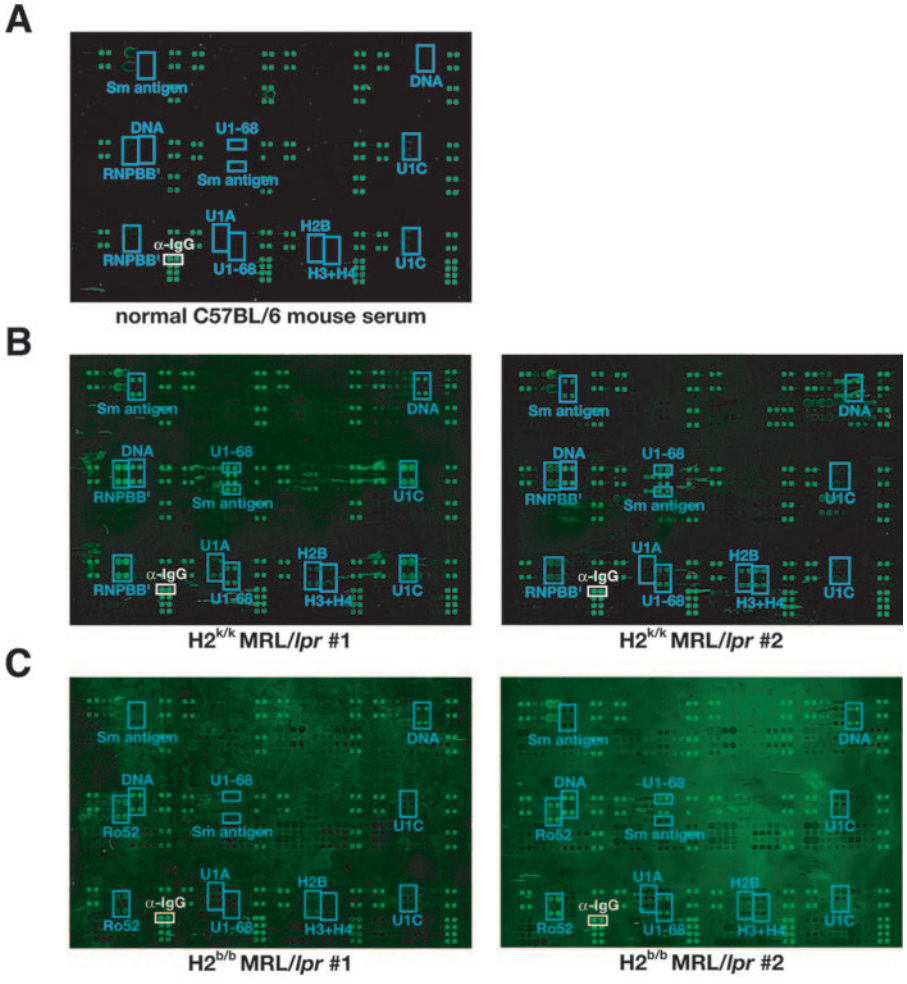

Antigen feature	normal C57BL/6	$H2^{k/k}$ #1	$H2^{k/k}$ #2	$H2^{b/b}$ #1	$H2^{b/b}$ #2
Sm antigen	7	1,717	1,829	1,431	958
DNA	8	11,089	3,891	3,693	6,651
U1snRNP-BB'	112	8,280	5,723	2,088	1,447
U1snRNP-68	39	4,927	2,698	2,344	2,979
U1snRNP-A	8	3,693	1,678	1,827	853
U1snRNP-C	41	7,377	1,350	2,042	1,253
Histone H2B	10	2,993	2,794	1,525	807
Histone H3+H4	14	2,513	1,570	2,661	405
Ro52	14	2,383	1,793	3,775	3,608
α-IgG	17,500	17,500	17,500	17,500	17,500

FIGURE 2. Connective tissue disease arrays. Ordered Ag arrays were produced using a robotic microarrayer to attach lupus-associated Ags and Abs directed against mouse IgG (α-IgG) to poly-L-lysine-coated microscope slides. Individual arrays were probed with diluted mouse sera. The positions of select autoantigens and control features are indicated. *A*, An array probed with normal control C57BL/6 mouse serum showed no autoantibody reactivity. *B*, Representative images of arrays probed with sera from two 20-wk-old F_9 $H2^{k/k}$ MRL/*lpr* mice. *C*, Representative images of arrays probed with sera from two F_9 $H2^{b/b}$ MRL/*lpr* mice. *D*, Quantitative analysis of *A–C*. Results are expressed as normalized DFU (see *Materials and Methods*).

Threshold parameters were selected so that negative control Ags were excluded and false discovery rates (q values) were ≤5%. Two-class SAM identified Ags with significant differences in reactivities between 20-wk-old $H2^{b/b}$ and $H2^{k/k}$ MRL/*lpr* mice. Thresholds for positive values included an absolute difference in normalized DFU between groups > 500 and a false discovery rate (q) of <0.05 (25). Ags meeting these criteria were designated as positive and selected for cluster analysis. Positive SAM hits were subjected to hierarchical clustering using Cluster software (26) and results displayed using TreeView software (26).

Autoantibody ELISA

Serum autoantibody levels against dsDNA and glomerular Ags (GA) were measured as described previously (27). For the anti-DNA ELISA, plates were coated overnight at 37°C with double-stranded calf thymus DNA (5 μg/ml; Sigma-Aldrich) diluted in SSC buffer. For the anti-GA ELISA, plates were coated for 90 min with rat GA (40 μg/ml) diluted in PBS. After washing, serum was added in serial dilutions starting at 1/100. Bound Abs were detected with HRP-conjugated goat anti-mouse IgG (γ-chain specific; Sigma-Aldrich) or anti-mouse IgG subclasses (Southern Biotechnology Associates) and developed with 3,3′,5,5′-tetramethylbenzidine (TMB; Sigma-Aldrich) solution. OD_{380} absorbance was measured as described previously. IgG3 anti-mouse IgG2a RF levels were measured by ELISA. Briefly, ELISA plates were coated with mouse IgG2a (1 μg/ml; Southern Biotechnology Associates) overnight. After washing, serum was added in serial dilutions starting at 1/100 dilution. The assay was then performed as described above with HRP-conjugated goat anti-mouse IgG3 (Southern Biotechnology Associates). Assays for histones were performed similarly. The anti-Sm ELISA was performed as described previously (28). Briefly, ELISA plates were coated with 10 U/ml Sm Ag (Immunovision) in borate-buffered saline (BBS) at 4°C overnight, washed, and blocked with BBS containing 1% BSA. Serum diluted in BBS-Tween 20/1% BSA was incubated in the plates for 2 h. The assay was then performed as described above with HRP-conjugated goat anti-mouse IgG or anti-mouse IgG subclasses, except for using BBS instead of PBS. Assays for snRNP were performed similarly (Immunovision).

Measurement of serum Ig isotype levels

Serum Ig levels were measured by ELISA. Briefly, microtiter plates were coated overnight at 4°C with goat anti-mouse Ig (M plus G plus A) (2 μg/ml; Southern Biotechnology Associates) or goat anti-mouse IgG (1 μg/ml; Southern Biotechnology Associates) diluted in 0.05 M carbonate-bicarbonate buffer (pH 9.6). Sera and Abs were diluted in

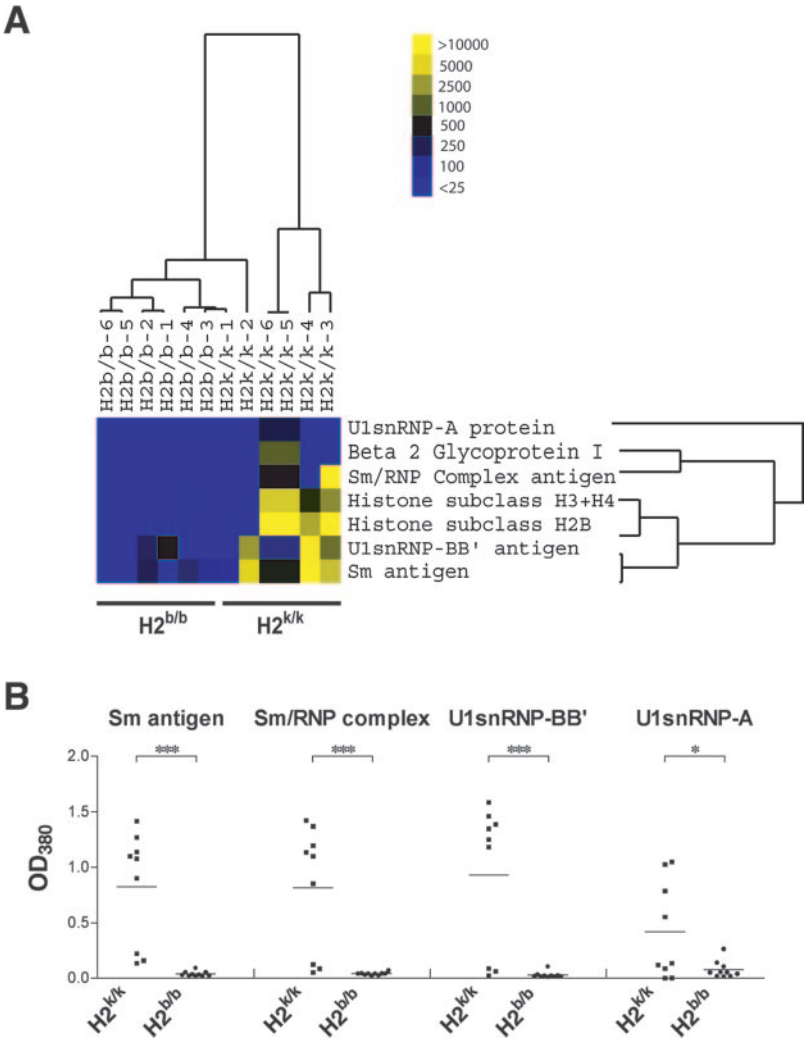

FIGURE 3. SAM and Cluster analysis with ELISA confirmation. *A*, Hierarchical clustering of Ag features with significant differences in reactivity between sera derived from F_9 $H2^{k/k}$ and $H2^{b/b}$ mice. SAM was used to identify features with significant differences in array reactivity between groups. A hierarchical cluster algorithm was applied to order mice based on similarities in their array reactivities for the SAM-identified features (dendrograms depicting cluster relationships are displayed above the individual mice) and to order Ag features based on similarities in reactivities in the mice studied (dendrograms displayed to the *right*). Relationships between mice or Ag features are represented by tree dendrograms, whose branch lengths reflect the degree of similarity in array reactivity determined by the hierarchical cluster algorithm. After clustering, labels were added below the figure to indicate clusters of MRL/*lpr* mice with different MHC haplotypes. *B*, Confirmatory ELISA on serum from 20-wk-old MRL/*lpr* $H2^{b/b}$ and $H2^{k/k}$ mice. The data presented are the individual OD readings with the bar representing the mean. *, $p < 0.05$; ***, $p < 0.001$.

PBS-Tween 20 (PBS-T) (0.05%) containing 1% BSA (PBS-T/1% BSA). Serum dilutions were then incubated in the coated wells for 1 h, and bound Abs were detected with HRP-conjugated anti-mouse IgM, IgG1, IgG2a, IgG2b, or IgG3 (Southern Biotechnology Associates) and developed with TMB (Sigma-Aldrich), 0.1 M citrate buffer (pH 4.0), and 0.015% H_2O_2. Purified mouse Ig isotypes (Southern Biotechnology Associates) were used as standards. Absorption at OD_{380} was determined on a flow microtiter plate reader (Dynatech Laboratories). Standard curves and serum Ab concentrations were calculated using DeltaSoft 3 (version 2.2; BioMetallics), and statistical analysis was performed with GraphPad Prism software (version 3.0; GraphPad).

ELISPOT assay

The number of IgM, IgG1, IgG2a, IgG2b, or IgG3 secreting cells in the spleen was assessed by ELISPOT. Ninety-six-well multiscreen plates (Millipore) were coated overnight with 1 μg/ml goat anti-mouse Ig (M plus G plus A; Southern Biotechnology Associates) in 0.05 M carbonate-bicarbonate buffer (pH 9.6) and then washed with endotoxin-free Dulbecco's PBS and blocked with 200 μl/well of PBS containing 3% BSA. The plates were washed with DMEM containing 3% BSA and incubated in triplicate with spleen cells in serial dilutions starting at 1×10^6 cells/well in 100 μl of DMEM with 3% BSA, 2.5% FCS, streptomycin, and penicillin. Following a 2-h incubation, the plates were washed with 1 M NaCl and PBS-T (0.25%). Then, the plates were incubated with 100 μl/well biotinylated goat anti-mouse IgM, IgG1, IgG2a, IgG2b, or IgG3 (each 0.5 μg/ml; Southern Biotechnology Associates) in 1% BSA/PBS-T, followed by 50 μl/well streptavidin-HRP (0.2 μg/ml; Jackson ImmunoResearch Laboratories). After washing, the plates were developed with 50 μl/well of a substrate solution containing 0.3 mg/ml 3-amino-9-ethylcarbazole (Sigma-Aldrich) in 0.05 M sodium acetate (pH 5.0) and 0.015% H_2O_2. The reaction was stopped by washing with tap water, and the number of spots were counted using a dissecting microscope.

Measurement of urine albumin excretion

Mice were placed in metabolic cages for 24-h urine collection every 2 wk beginning at 12 wk of age. Urinary albumin excretion was determined by ELISA using a standard curve of known concentrations of mouse albumin (Cappel). Briefly, 96-well ELISA plates were coated with 2.5 μg/ml goat anti-mouse albumin (Research Diagnostics) overnight at 4°C. After washing with PBS-T, PBS-0.25% gelatin (Sigma-Aldrich) was added to each well to block nonspecific binding. Urine samples were added in serial dilutions, starting at a 1/10 dilution, and incubated for 1 h at room temperature. After washing with PBS-T, HRP-conjugated goat anti-mouse albumin (Research Diagnostics) was added. After additional washing, the plates were developed with TMB solution, and urine albumin concentration was calculated using DeltaSoft 3 (version 2.2; BioMetallics), and statistical analysis was performed with GraphPad Prism software (version 3.0; GraphPad). Data are reported as milligrams of albumin/mouse/day.

Renal pathology

At the time of sacrifice (32 wk of age), the kidneys were removed. One kidney was fixed with 10% buffered formalin, embedded in paraffin, then sectioned before staining with H&E. The other half kidney was snap-frozen in liquid nitrogen and placed in OCT medium. Four-micrometer-thick frozen sections were stained with fluorescein-conjugated anti-mouse total IgG, IgG3 (Southern Biotechnology Associates), or C3 (Cappel). The remaining kidney was diced into small pieces (~2 mm), dipped in glycolaldehyde buffer, and prepared for electron microscopy (EM) analysis by standard procedure. The H&E kidney slides were graded for glomerular inflammation, proliferation, crescent formation, and necrosis. Scores from

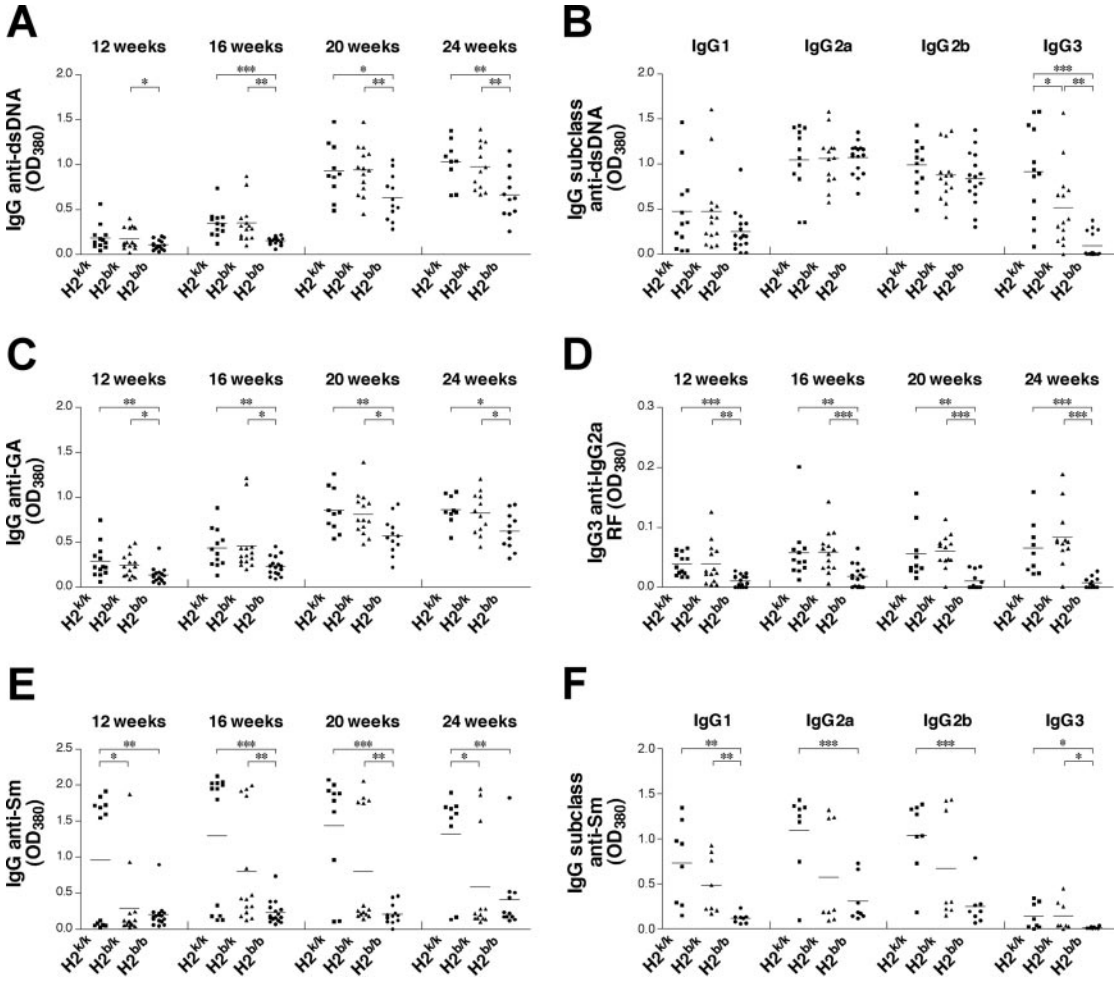

FIGURE 4. Serum autoantibodies in MRL/*lpr* mice. Serum IgG anti-dsDNA (*A*), IgG anti-GA (*C*), IgG3 anti-mouse IgG2a RF (*D*), and IgG anti-Sm (*E*) levels in the F_9 $H2^{k/k}$, $H2^{b/k}$, and $H2^{b/b}$ MRL/*lpr* mice were measured by ELISA. $n = 12$–16 in each group at 12 wk of age. The number of the mice in each group decreased with aging due to mortality. Twenty-week-old mice sera from each group were used for IgG subclass analysis of anti-dsDNA (*B*) and anti-Sm (*F*) Abs. *, $p < 0.05$; **, $p < 0.01$; ***, $p < 0.001$.

0 to 3+ (0, none; 1+, mild; 2+, moderate; 3+, severe; scores of crescent formation and necrosis were doubled) were assigned for each of these features and then added together to yield a final renal score. Immunofluorescence slides were graded 0 to 3+ (0, none; 1+, mild staining; 2+, moderate staining; 3+, high staining) for fluorescence intensity. EM samples were assessed for morphological changes of glomerular cells, glomerular immune electron-dense deposit localization (i.e., mesangial, subendothelial, and subepithelial deposition) and podocyte foot process fusion, and were graded 0 to 3+ (0, none; 1+, mild; 2+, moderate; 3+, severe). All pathological assessments were performed in a blinded fashion.

Statistics

The unpaired Student's *t* test was used to test for significant differences between groups. The Mann-Whitney two-tailed *U* test or Kruskal-Wallis test was used to determine the significance of changes in glomerular IgG, IgG3, and C3 deposition (see Fig. 6*B*), renal score (see Fig. 6*C*), and glomerular electron-dense deposits (see Fig. 6*D*). A value of $p < 0.05$ was considered significant.

Results

Generation of study mice

129/Sv ($H2^b$) mice were backcrossed for nine generations to MRL/*lpr* mice. After nine generations of backcrossing, $H2^{b/k}$ heterozygous MRL/*lpr* mice were intercrossed to obtain F_9 $H2^{k/k}$, $H2^{b/k}$, and $H2^{b/b}$ MRL/*lpr* mice. The termini of the $H2^b$ interval of F_9 congenic MRL/*lpr* mice were mapped with microsatellite markers located near the selected four H2 markers. As shown in Fig. 1, the $H2^b$ interval extended 1 cM centromeric of *D17Mit16* and 0.5 cM telomeric of *D17Mit177*. Thus, the centromeric crossover point on H2 was between *D17Mit198* (16.0 cM) and *D17Mit61* (16.4 cM), and the telomeric crossover point was between *D17Mit65* (24.5 cM) and *D17Mit108* (24.7 cM). Extensive genotyping to confirm lack of recombinational events in H2 and to exclude admixture outside of the H2 is detailed in *Materials and Methods* and summarized in Fig. 1. Phenotypic confirmation of genetic markers was determined by flow cytometric analysis of H2 class I (K) and class II (I-A, and I-E) expression on PBMC from mice of each F_9 $H2^{k/k}$, $H2^{b/k}$, and $H2^{b/b}$ MRL/*lpr* strain (data not shown).

To assess the effect of H2 haplotype on disease expression in MRL/*lpr* mice, we evaluated the mice biweekly for development of skin rash, ear necrosis, and lymphadenopathy beginning at 8 wk of age until the time of sacrifice (32 wk old; $n = 12$–16 in each group). No differences were observed between the three groups in these external manifestations of disease (data not shown). At the time of sacrifice, there were no differences in body weight or spleen weight between the three groups (data not shown).

Serum autoantibody assays

To assess the effect of H2 haplotype on the spectrum of autoantibody production in MRL/*lpr* mice, we used recently developed

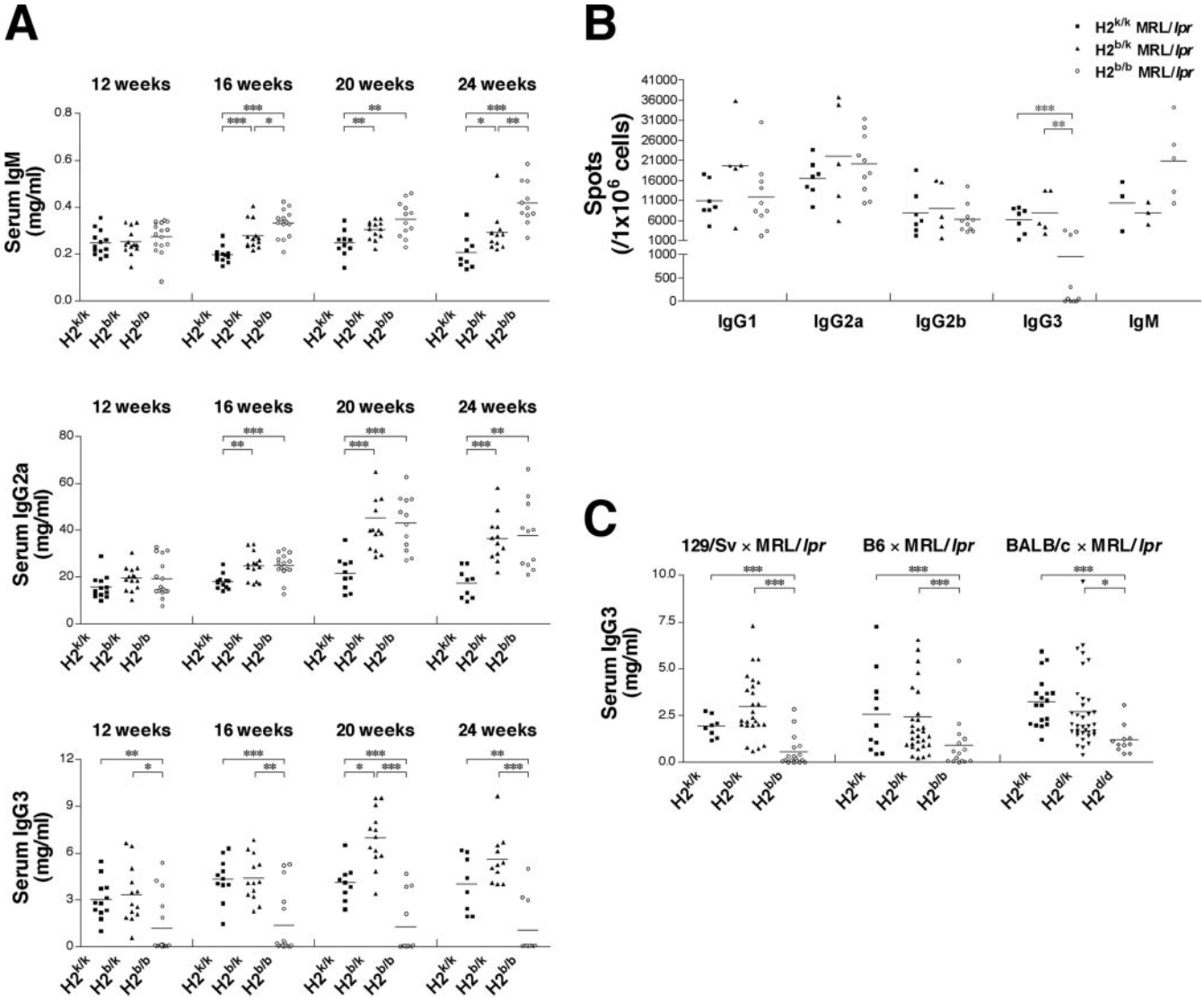

FIGURE 5. Serum Ig levels and Ab-producing cells in MRL/*lpr* mice. *A*, Serum concentrations of IgM (*upper panel*), IgG2a (*middle panel*), and IgG3 (*lower panel*) in the 129/Sv strain-derived F_9 $H2^{k/k}$, $H2^{b/k}$, and $H2^{b/b}$ MRL/*lpr* mice were determined by ELISA using standards of known concentration. Eleven of 16 (68.8%) of the $H2^{b/b}$ MRL/*lpr* mice had undetectable serum IgG3 levels. $n = 12$–16 mice in each group at 12 wk of age. The number of the mice in each group decreased with aging due to mortality. *, $p < 0.05$; **, $p < 0.01$; ***, $p < 0.001$. *B*, Populations of Ig isotype producing cells in the spleens of 32-wk-old F_9 $H2^{k/k}$, $H2^{b/k}$, and $H2^{b/b}$ MRL/*lpr* mice. The F_9 H2 MRL/*lpr* mice were sacrificed at 32 wk, and spleen cells were analyzed by ELISPOT assay. $n = 7$ in the $H2^{k/k}$, 5 in the $H2^{b/k}$, and 10 in the $H2^{b/b}$ MRL/*lpr* mice for IgG isotype analysis. $n = 3$, 3, and 5 in the $H2^{k/k}$, $H2^{b/k}$, and $H2^{b/b}$ MRL/*lpr* mice for IgM-producing cell analysis, respectively. **, $p < 0.01$; ***, $p < 0.001$. *C*, Serum concentrations of IgG3 in 12-wk-old 129/Sv, B6, or BALB/c strain-derived F3 $H2^{k/k}$, $H2^{b/k}$, $H2^{b/b}$, $H2^{d/k}$, and $H2^{d/d}$ MRL/*lpr* mice were determined by ELISA using standards of murine IgG3 of known concentration. *, $p < 0.05$; ***, $p < 0.001$.

autoantigen microarray technology. Using 1152-feature arrays composed of 140 Ags or Ag fragments, we analyzed serum derived from six different $H2^{b/b}$ and $H2^{k/k}$ mice at 20 wk of age. Arrays were scanned and images analyzed as described in *Materials and Methods*. The data sets were analyzed using the SAM algorithm, applying highly stringent false discovery rates (5%) as cutoffs. Using these criteria, SAM identified seven Ags (U1snRNP-A, U1snRNP-BB′, Sm/RNP complex, Sm Ag, β-2-glycoprotein I, histone H2B, and histone H3+H4) that were differentially recognized by sera from $H2^{k/k}$ compared with $H2^{b/b}$ MRL/*lpr* mice (Figs. 2 and 3). To confirm these findings, ELISA for these Ags were performed. Although the Ags used in the microarray experiments were the same as those used for the confirmatory ELISA, the differences between the two groups in serum levels of Abs to β-2-glycoprotein I, histone H2B, and histone H3+H4, although present, were not significant when analyzed by ELISA (data not shown). However, microarray results for four of the Ags—U1snRNP-A, U1snRNP-BB′, Sm/RNP complex, and Sm Ag—were validated by ELISA (Fig. 3*B*). These results indicate a profound effect of MHC on autoantigen selection in MRL/*lpr* mice. These results also demonstrate that autoantigen arrays are a useful tool for discovery of novel autoantibody reactivities in murine SLE; testing that is impractical for individual Ags by ELISA techniques.

Serum anti-dsDNA Ab, anti-GA Ab, and IgG3 RF with cryoglobulin activity are major nephritogenic autoantibodies in MRL/*lpr* mice (20, 29, 30). To determine whether H2 impacts the serum levels of key pathogenic autoantibodies in MRL/*lpr* mice, we analyzed serum levels of these autoantibodies by ELISA. Although serum from all animals contained anti-dsDNA and

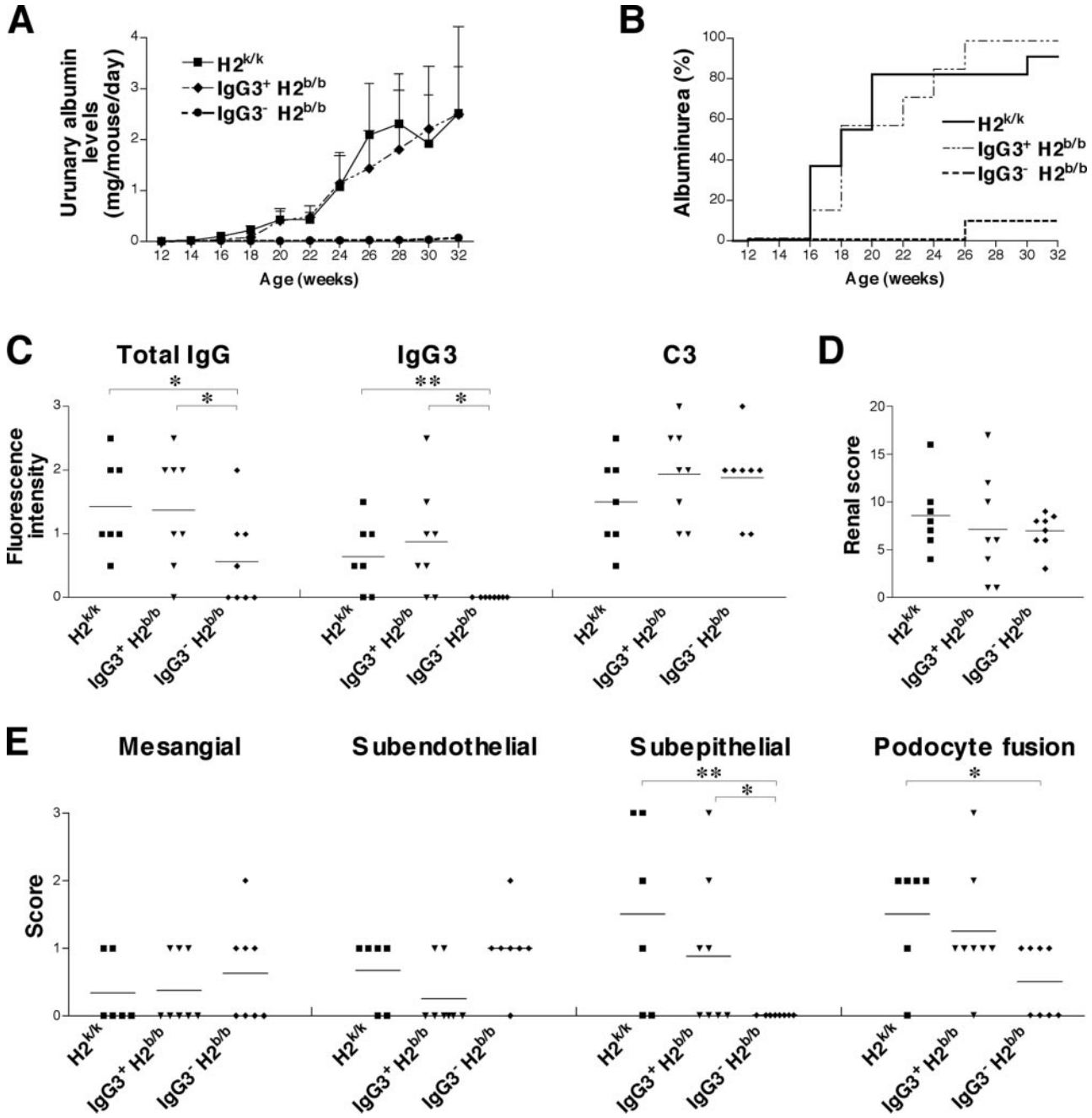

FIGURE 6. Renal disease assessment in MRL/*lpr* mice. *A*, Urinary albumin excretion levels in the $H2^{k/k}$, $IgG3^+$ $H2^{b/b}$, and $IgG3^-$ $H2^{b/b}$ MRL/*lpr* mice. Data presented are the mean 24-h albumin excretion (mg/mouse/day) ± SEM in each group. $n = 11$, 8, and 11 in the $H2^{k/k}$, $IgG3^+$ $H2^{b/b}$, and $IgG3^-$ $H2^{b/b}$ MRL/*lpr* mice, respectively. *B*, Albuminuria development (Kaplan-Meier curve) in the $H2^{k/k}$, $IgG3^+$ $H2^{b/b}$, and $IgG3^-$ $H2^{b/b}$ MRL/*lpr* mice. Mice excreting urinary albumin (>0.1 mg/mouse/day) were counted until the time of sacrifice (32 wk). $n = 11$, 8, and 11 in the $H2^{k/k}$, $IgG3^+$ $H2^{b/b}$, and $IgG3^-$ $H2^{b/b}$ MRL/*lpr* mice, respectively. Albuminuria in $H2^{b/k}$ mice was similar to the $IgG3^+$-producing groups (data not shown). *C*, Immunofluorescence assessment of glomerular IgG, IgG3, or C3 deposition of 32-wk-old MRL/*lpr* mice. *D*, Pathologic renal scores of 32-wk-old MRL/*lpr* mice. *E*, Glomerular immune electron-dense deposit localization and podocyte foot process fusion. EM analysis revealed no glomerular subepithelial dense deposits and reduced levels of foot process fusion in the $IgG3^-$ $H2^{b/b}$ MRL/*lpr* mice. $n = 6$–8 in each group. *, $p < 0.05$; **, $p < 0.01$.

anti-GA Abs, levels were significantly decreased in the $H2^{b/b}$ MRL/*lpr* mice compared with the other two groups (Fig. 4, *A* and *C*). We next analyzed anti-dsDNA levels of each IgG isotype and found that IgG3 was the only IgG anti-dsDNA isotype that was reduced in the $H2^{b/b}$ MRL/*lpr* mice (Fig. 4*B*). Serum IgG3 anti-IgG2a RF levels were also significantly lower in the $H2^{b/b}$ MRL/*lpr* mice compared with the other two groups (Fig. 4*D*), similar to our findings in the factor B-deficient MRL/*lpr* mice (31). These results suggested that lower levels of anti-dsDNA Ab, anti-GA Ab, and IgG3 anti-IgG2a RF in the $H2^{b/b}$ MRL/*lpr* mice were due to IgG3 deficiency alone.

To determine whether the lack of serum anti-Sm levels in the $H2^{b/b}$ MRL/*lpr* mice was also due to decreased IgG3 alone, we analyzed serum anti-Sm levels for each IgG isotype. We found none of the $H2^{b/b}$ MRL/*lpr* mice had anti-Sm Abs of any IgG isotype above background, whereas the $H2^{k/k}$ MRL/*lpr* mice had

detectable levels of serum anti-Sm Abs of each IgG isotype (Fig. 4, *E* and *F*), indicating that lower serum anti-Sm levels in the $H2^{b/b}$ MRL/*lpr* mice was not due to IgG3 deficiency alone.

Serum Ig levels

Given the effects of H2 on specific IgG isotype levels of anti-DNA Abs, we determined whether global serum Ig levels were affected by H2 genotype in the MRL/*lpr* strain. Serum IgM levels were statistically higher in the $H2^{b/b}$ MRL/*lpr* mice compared with the $H2^{k/k}$ and $H2^{b/k}$ groups (Fig. 5*A*, *upper panel*). Levels of serum IgG2a, the dominant IgG isotype in the serum of MRL/*lpr* mice (18), were also significantly higher in the $H2^{b/b}$ compared with $H2^{k/k}$ MRL/*lpr* mice (Fig. 5*A*, *middle panel*). Strikingly, 11 of the 16 $H2^{b/b}$ MRL/*lpr* mice had undetectable levels of serum IgG3 (Fig. 5*A*, *lower panel*), similar to our prior findings in MRL/*lpr* factor B-deficient mice (31). To confirm whether serum Ig isotype levels reflect the population of each Ig isotype-producing cell, we analyzed the population of each Ig isotype-producing cell in the spleen of F_9 $H2^{k/k}$, $H2^{b/k}$, and $H2^{b/b}$ MRL/*lpr* mice by ELISPOT analysis. As shown in Fig. 5*B*, 7 of 10 $H2^{b/b}$ MRL/*lpr* mice had no or very few ($0–50/1 \times 10^6$ spleen cells) IgG3-producing cells in the spleen, whereas it was a readily evident in the spleen of $H2^{k/k}$ and $H2^{b/k}$ MRL/*lpr* mice as well as other Ig isotype-producing cells. Although it did not reach statistical differences, there was a trend toward increased numbers of IgM- or IgG2a-producing cells in the spleen of $H2^{b/b}$ MRL/*lpr* mice compared with $H2^{k/k}$ MRL/*lpr* mice. These results of ELISOPT analysis were consistent with the results of serum Ig measurement.

To verify that IgG3 deficiency was due to the $H2^b$ haplotype, we analyzed serum IgG3 levels in F_3 B6 strain-derived $H2^b$ ($H2^b$·B6) and BALB/c strain-derived $H2^d$ ($H2^d$·BALB/c) MRL/*lpr* mice. The F_3 $H2^{b/b}$·B6 MRL/*lpr* mice had significantly decreased serum IgG3, with 7 of 15 being totally deficient (Fig. 5*C*). F_3 $H2^{b/b}$·129/Sv MRL/*lpr* mice also had significantly decreased serum IgG3 levels (Fig. 5*C*). Serum derived from F_3 $H2^{d/d}$·BALB/c MRL/*lpr* mice had lower levels of serum IgG3 than $H2^{k/k}$ MRL/*lpr* mice; however, unlike $H2^{b/b}$ MRL/*lpr* mice, no $H2^{d/d}$ MRL/*lpr* mice were completely deficient in serum IgG3 (Fig. 5*C*). From these results, we concluded that the combination of $H2^b$ haplotype and unidentified genes within the MRL/*lpr* genetic background result in the observed deficiency in IgG3 production in 70% of $H2^b$ MRL/*lpr* mice.

Assessment of glomerulonephritis

IgG3 autoantibodies are reported to be pathogenic in glomerulonephritis in MRL/*lpr* mice (18, 20), and thus, we hypothesized that the IgG3-deficient mice would have less renal disease and vasculitis than their IgG3-producing littermates. We separated the $H2^{b/b}$ MRL/*lpr* mice into IgG3-producing mice ($IgG3^+$) and IgG3-deficient mice ($IgG3^-$). To assess the development of glomerulonephritis, we measured 24-h urinary albumin excretion by ELISA beginning at 12 wk of age (Fig. 6, *A* and *B*). Albuminuria was first observed in the IgG3-producing groups (the $H2^{k/k}$, $H2^{b/k}$, and $IgG3^+$ $H2^{b/b}$ mice) at 16–18 wk of age, and there was no difference among the three groups (data for the $H2^{b/k}$ MRL/*lpr* mice are not shown). In contrast to the IgG3-producing mice, 10 of 11 $IgG3^-$ $H2^{b/b}$ MRL/*lpr* mice did not develop albuminuria (>0.1 mg/mouse/day) through 32 wk of age.

Mice in all groups were sacrificed at 32 wk (seven $H2^{k/k}$, eight $IgG3^+$ $H2^{b/b}$, and eight $IgG3^-$ $H2^{b/b}$ mice), and histopathologic analysis was performed. Immunofluorescence staining revealed that the $IgG3^-$ $H2^{b/b}$ MRL/*lpr* mice had significantly less glomerular IgG deposition compared with the $H2^{k/k}$ and $IgG3^+$ $H2^{b/b}$ MRL/*lpr* mice (Figs. 6*C* and 7*A*). As expected, there was no IgG3 detected in the glomeruli of the serum $IgG3^-$ mice, whereas it was readily evident in the glomeruli of the serum $IgG3^+$ mice (Figs. 6*C* and 7*A*). In contrast to the reduction in albuminuria and glomerular immune complex deposition in the $IgG3^-$ mice, there was no significant difference in glomerular C3 deposition. In contrast to our predictions based on the pathogenicity of IgG3 autoantibodies, there was no significant difference in pathologic renal scores between the groups assessing glomerular disease and vasculitis (Figs. 6*D* and 7*A*).

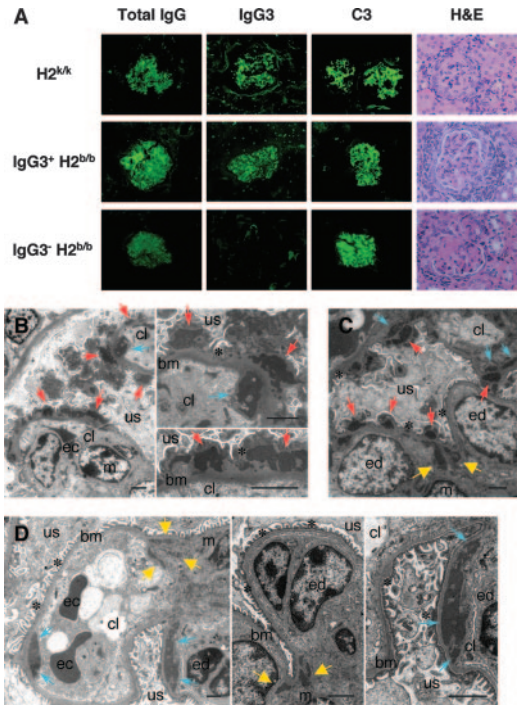

FIGURE 7. Histological, immunofluorescence, and EM studies of kidneys from MRL/*lpr* mice. *A*, Representative sections of kidneys from MRL/*lpr* mice differing in H2 and IgG3 production. Total IgG, IgG3, and C3 glomerular deposition as assessed by immunofluorescence are depicted in the *left three panels*. Proliferative glomerular disease and inflammation are demonstrated in H&E-stained paraffin sections. *B–D*, EM analysis of kidneys from F_9 $H2^{k/k}$ (*B*), $IgG3^+$ $H2^{b/b}$ (*C*), and $IgG3^-$ $H2^{b/b}$ (*D*) MRL/*lpr* mice. Both the $H2^{k/k}$ and $IgG3^+$ $H2^{b/b}$ mice had extensive subepithelial (red arrows), subendothelial (blue arrows), and mesangial (yellow arrows) electron-dense deposits, a thickened GBM (bm), and extensive fusion of podocyte foot processes (*). In contrast, in the glomeruli of the $IgG3^-$ $H2^{b/b}$ MRL/*lpr* mice, there were subendothelial and mesangial dense deposits, but no subepithelial deposits and little or no basement membrane thickening or foot process fusion. Each image is representative of the results obtained from one kidney of six to eight mice per group. us, urinary space; cl, capillary lumen; ed, endothelial cell; m, mesangial cell; and ec, erythrocyte. Scale bars, 2 μm.

To investigate the discrepancy between albuminuria, glomerular immune complex deposition, and renal score, we performed EM analysis on renal sections from all groups. The $IgG3^-$ $H2^{b/b}$ MRL/*lpr* mice had electron-dense deposits in the glomerular subendothelial space and mesangial matrix similar to the $IgG3^+$ groups (Figs. 6*E* and 7, *B–D*). Notably, none of the sections from $IgG3^-$ $H2^{b/b}$ mice had glomerular subepithelial deposits. Such deposits were readily evident in glomeruli from mice in the $IgG3^+$ groups regardless of H2 haplotype (Figs. 6*E* and 7, *B–D*). Furthermore, podocyte foot process fusion was significantly more evident in the $IgG3^+$ $H2^{k/k}$ mice compared with the $IgG3^-$ $H2^{b/b}$ mice (Figs. 6*E* and 7, *B–D*).

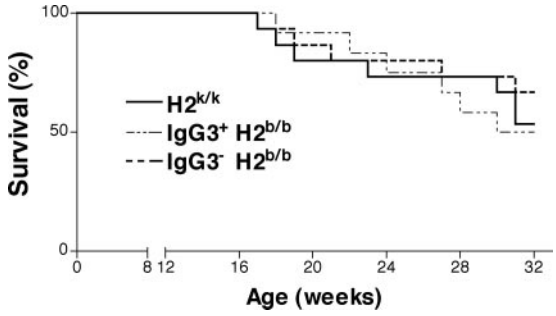

FIGURE 8. Survival of MRL/*lpr* mice differing in H2 and IgG3 production. Mortality was observed until the time of sacrifice (32 wk). There were no differences in survival between the groups. $n = 13–16$ in each group.

We also assessed a limited number of IgG3$^+$ H2$^{b/k}$ MRL/*lpr* mice ($n = 3$) and observed intermediate changes compared with pathological features observed in H2$^{k/k}$ and H2$^{b/b}$ MRL/*lpr* mice (data not shown). These EM changes likely explain most of the differences in proteinuria between the groups.

Survival

Thirteen to 16 mice in each F_9 MRL/*lpr* H2 congenic group (H2$^{k/k}$, H2$^{b/k}$, IgG3$^+$ H2$^{b/b}$, and IgG3$^-$ H2$^{b/b}$ MRL/*lpr* mice) were observed for spontaneous mortality until the time of sacrifice (32 wk). Despite the significant differences in serum autoantibodies, glomerular immune complex deposition, and albuminuria, there was no difference in survival among the groups likely reflecting the similarities in proliferative renal disease in the three groups (Fig. 8; data of H2$^{b/k}$ mice is not shown).

Discussion

The data presented herein indicate that gene(s) encoded within or closely linked to the MHC region regulates autoantibody targeting of specific autoantigens in MRL/*lpr* mice and IgG3 isotype switching. The critical role of IgG3 in localization of glomerular immune complex deposits and subsequent proteinuria in MRL/*lpr* mice was an additional novel finding in these studies. The final novel observation is that despite these profound effects on disease parameters, including the lack of IgG3, H2 did not impact the development of proliferative renal disease, vasculitis, or survival of MRL/*lpr* mice.

An intriguing result in comparing H2^b and H2^k MRL/*lpr* mice was the stark difference in autoantibody specificity. Protein microarrays were only recently applied to the study of autoimmune disease, particularly to large-scale autoantibody profiling. Robinson et al. (22) demonstrated the use of autoantigen microarrays for measuring human autoantibodies that characterize eight distinct systemic rheumatic diseases. These studies were extended to two other animal models of human disease: the experimental autoimmune encephalomyelitis model of multiple sclerosis (32) and a monkey model of acquired immunodeficiency syndrome (33), as well as to the study of human patients with rheumatoid arthritis (34). Zhen et al. (35) recently reported the discovery of predictive autoantibody profiles in a congenic mouse model of SLE, further suggesting that multiplex autoantibody profiling might aid in uncovering pathogenic mechanisms that contribute to SLE pathogenesis.

In the current study, we used the previously validated connective tissue disease arrays (22) as a discovery tool to identify differences in autoantibody production between groups of animals expressing unique H2 haplotypes. This led to the novel discovery that a subset of prominent SLE autoantigens are frequently targeted in H2$^{k/k}$ but are completely absent in H2$^{b/b}$ MRL/*lpr* mice. It is unlikely that all these differences would have been identified using low-throughput assays such as ELISA to screen the hundreds of known candidate SLE Ags. Thus, these results demonstrate the use of autoantigen microarray technology as a discovery tool.

The differences between the H2$^{k/k}$ and H2$^{b/b}$ groups in serum levels of autoantibodies to three SAM-identified Ags—β-2-glycoprotein I, histone H2B, and histone H3+H4—although present, were not statistically significant when analyzed by ELISA. However, it is worth noting that autoantigen arrays offer the ability to detect reactivity to autoantigens with sensitivity that is potentially superior to ELISA (22). The SAM algorithm was originally developed for analysis of DNA microarray data, and it has proven useful recently in the analysis of autoantigen array data (33, 34). SAM is capable of detecting differences between groups, which, although subtle, may nevertheless be clinically relevant. Analysis of larger numbers of samples for those Ags identified as significant by SAM will be required to directly test the validity of the algorithm. The current generation arrays are being expanded to include overlapping peptides with a goal to identify epitopes that we predict might bind to disease-specific MHC gene products.

In this study, both protein microarray analysis and conventional ELISA clearly demonstrated strong recognition of Sm Ag and snRNP proteins by sera from H2$^{k/k}$ MRL/*lpr* mice, whereas none of the H2$^{b/b}$ MRL/*lpr* mice had reactivity to these Ags above background activity in serum of BALB/c mice. Abs to Sm Ag are currently regarded as the most specific, although insensitive, marker of SLE. Abs to snRNP are also observed in sera from lupus patients, but they are present in much higher titers in sera from patients with mixed connective-tissue disease (36). Abs to Sm Ag and snRNP Ags are often linked in both patients and murine models of lupus (37). Our results indicate that gene(s) encoded within or closely linked to the MHC region (i.e., H2^b interval in H2 congenic mice) regulates anti-Sm/RNP production in MRL/*lpr* mice. Indeed, in previous studies of MHC and human lupus, it has been suggested that reactivity to major autoantigens (Ro (SS-A), La (SS-B), ribosomal P, β-2-glycoprotein I, Sm Ag, and U1-RNP) is linked with HLA class II alleles (DQ and DR), except for antinuclear Ab and anti-ssDNA (38, 39). HLA class II haplotypes carrying certain HLA-DR2 and -DR3 (and their linked HLA-DQ alleles) also have been associated with susceptibility to SLE. However, HLA class II alleles show stronger associations with specific autoantibody responses than with lupus itself or clinical features thereof (40). An association between HLA class II alleles and specific autoantibody generation is consistent with the concept of an Ag-driven process involving Th cell recognition. In previous studies of MHC and murine lupus, autoantibody production and lupus susceptibility were linked to the class II I-E-deficient haplotype carried in H2^b mice in BXSB (41), (NZB $\times$ BXSB)F_1 (42, 43), (MRL $\times$ BXSB)F_1 (44), and B6/*lpr* mice (37). I-Eα, which is a homolog of human DRα-chain, is deficient in H2^b mice due to a deletion of the promoter region of the *Ea* gene (45). In contrast to these studies, we found no accelerated autoantibody production in the I-E$^-$ H2$^{b/b}$ MRL/*lpr* mice. Indeed, there were reduced autoantibody levels and a more limited autoantibody spectrum in the I-E$^-$ H2$^{b/b}$ compared with the I-E$^+$ H2$^{k/k}$ mice. Whether the observed differences in autoantibody specificity in this study are directly linked to I-E deficiency or other uncharacterized differences between H2^k and H2^b remains to be determined.

IgG3 deficiency accounts for some of the autoantibody differences between the H2$^{b/b}$ and H2$^{k/k}$ mice (i.e., anti-dsDNA and

IgG3 RF) but not all (i.e., the anti-Sm Ag response). Our results also differ from a recent study of the effect of the $H2^b$ genotype on the Fas-intact $MRL^{+/+}$ $H2^k$ strain (46). Similar to our findings, Kong et al. (46) observed decreased levels of anti-dsDNA Abs, although they did not perform Ig isotype analysis. In contrast to our findings, these investigators did not observe differences in anti-U1-snRNP Abs between the H2 disparate strains. These contrasting findings may reflect differential effects of H2 on Fas-intact vs Fas-deficient strains and/or the enhanced sensitivity of the protein microarrays.

A prior study using F2 intercrosses of MRL/*lpr* and B6/*lpr* mice demonstrated four non-MHC-linked lupus susceptibility loci—"*Lmb1*, *-2*, *-3*, and *-4*,"—that localized to chromosomes 4, 5, 7, and 10, respectively (10). *Lmb1*, *-2*, and *-3* were linked to the production of anti-dsDNA Abs, but not glomerulonephritis, whereas *Lmb4* was associated with glomerulonephritis. No significant links between autoantibody production or pathologic disease and H2 were reported in this study. The authors did not, however, assess proteinuria, serum IgG isotypes, or anti-Sm/RNP Abs.

Despite significant differences in serum autoantibody levels, there was no difference in pathologic renal scores between $H2^{k/k}$ and $H2^{b/b}$ MRL/*lpr* mice, suggesting circulating autoantibodies do not directly correlate with proliferative renal disease in MRL/*lpr* mice. Our results are consistent with the observations of Chan et al. (47) that serum autoantibodies are not required for full development of renal disease in MRL/*lpr* mice. Our results, taken together with these previous reports, suggest that the $H2^b$ genotype has minimal effect on production of nephrogenic autoantibodies, proliferative glomerulonephritis, or mortality in MRL/*lpr* mice. However, H2 does influence the selection of autoantigens for autoantibody targeting.

The association of MHC haplotype with IgG isotype spectrum is not well understood. Recently, an association between H2 haplotype and serum IgG2a levels was demonstrated in H2 congenic B10 and BALB/c mice (48, 49). The phenotypic marker of high IgG2a levels, denoted Ig isotype-1 (*Igis1*), was mapped to the central MHC class III region. Linkage of specific Ab isotype deficiency with the MHC is also present in humans (50, 51). It is unclear whether the previous reports and our findings are caused by common or independent gene(s). It is possible that we are describing common gene(s) that affect isotype switching to either IgG3 or IgG2a depending on interactions with other background genes.

In our study, it is unclear why most, but not all, F_9 $H2^{b/b}$ MRL/*lpr* mice (>99.8% MRL/*lpr* background) had undetectable levels of serum IgG3. Analysis of IgG3 production within litters suggested that IgG3 deficiency in $H2^{b/b}$ MRL/*lpr* mice was stochastic in nature. Mice within a litter were $IgG3^+$ or $IgG3^-$ regardless of the IgG3-producing status of their parents (data not shown). The "random" deficiency of IgG3 production in the majority of MRL/*lpr* $H2^b$ mice is similar to the stochastic control of the anti-Sm response in MRL/*lpr* $H2^k$ mice (52).

Previous studies implicated IgG3 autoantibodies in renal disease in MRL/*lpr* mice. Indeed, IgG3 Abs are the predominant isotype eluted from diseased MRL/*lpr* kidneys (18). Additionally, IgG3 anti-IgG2a RF derived from MRL/*lpr* mice induced glomerulonephritis when injected into normal mice (53, 54). In our study, IgG3 anti-IgG2a RF levels were significantly lower in $H2^{b/b}$ MRL/*lpr* mice due to the lack of IgG3 production. We predicted that the IgG3-deficient mice would have less severe proliferative renal disease, lack vasculitis, and have improved survival based on previous studies linking longevity of survival MRL/*lpr* mice with decreased production of IgG3 (19, 20). It is possible that if we sacrificed mice at an earlier time point, we may have detected differences between the groups; however, the similar survival in the three groups suggests that any differences would not have been clinically relevant. Based on our results, we believe that, although IgG3 autoantibodies may be sufficient to induce proliferative renal disease and vasculitis in MRL/*lpr* mice, they are not required for proliferative renal disease development or vasculitis and have no effect on survival.

Of interest in our study, the $IgG3^-$ $H2^{b/b}$ MRL/*lpr* mice had significantly reduced albuminuria but had renal scores and survival similar to $IgG3^+$ littermates, regardless of H2 genotype. This observation indicates that the presence and/or amount of albuminuria does not necessarily parallel or predict the severity of proliferative renal disease as the $IgG3^-$ mice developed proliferative glomerulonephritis despite minimal proteinuria. To gain insight into the mechanisms underlying reduced albuminuria in the $IgG3^-$ mice, we performed EM analysis. The $IgG3^-$ $H2^{b/b}$ MRL/*lpr* mice, which had low levels of albuminuria, had electron-dense immune deposits in the subendothelial space of the glomerular capillary wall, but not in the subepithelial area. The $IgG3^+$ MRL/*lpr* mice, which developed severe albuminuria, had electron-dense deposits in the subepithelial space, as well as in the subendothelial areas. In murine models of nephrotic syndrome and in human nephrotic syndrome, where proteinuria is a key measure of disease, subepithelial immune deposits, and podocyte foot process effacement are a near universal finding (55). In our results, the extent of podocyte foot process effacement was significantly less in the $IgG3^-$ MRL/*lpr* mice compared with the $IgG3^+$ MRL/*lpr* mice. In these models and human kidney disease, the occurrence and severity of proteinuria and podocyte effacement is associated with the presence of glomerular subepithelial electron-dense deposits (56–58). The severity of proliferative renal disease in lupus nephritis, however, correlates with the presence of subendothelial deposits that were similar in the different MRL/*lpr* H2 groups (56, 59). The mechanisms of immune deposition on, and transport through, the glomerular basement membrane (GBM) are largely unknown. Our results suggest that IgG3 plays an important role in the specific localization of immune deposits in the kidneys of MRL/*lpr* mice and secondarily in the development of proteinuria. How IgG3 influences the location of immune complex deposition and subsequent albuminuria remains unclear. In MRL/*lpr* mice, IgG3 is the only IgG subclass that exhibits a cationic shift between isoelectric point 7.5 and 8.0 in isoelectric focusing (18). The initial deposition of cationic IgG3 immune complexes in the subendothelial space may interfere with the negatively charged selective barrier of the GBM by electrical neutralization. This may allow immune complexes to pass through the GBM to the subepithelial space where they can induce podocyte effacement and subsequent protein leakage into the urinary space. The influence of IgG3 on complement activation and/or FcR activation may also play a role in immune complex localization (60–62).

In conclusion, our results demonstrate that in MRL/*lpr* mice: 1) there are striking differences in autoantibody specificity for nuclear protein Ags between MRL/*lpr* $H2^b$ and $H2^k$ mice, identified by microarray screening techniques; 2) $H2^b$ expressed on the MRL/*lpr* background leads to IgG3 deficiency in the majority of mice, a finding that is likely due to complex genetic interactions; 3) IgG3 plays an important role in determining localization of glomerular immune complex deposits and secondarily excretion of albumin into the urine; and 4) IgG3 autoantibodies are not necessary for development of proliferative renal disease or vasculitis in MRL/*lpr* mice and do not impact survival. These studies provide a novel

insight into the role of MHC in autoantigen selection and in the disease association of IgG3 with lupus nephritis. Additional studies are planned to define the genetic factors in H2 that control autoantigen selection, the genetic factors in H2 that control isotype switching to IgG3, and the mechanistic role of IgG3 in immune complex localization in the glomerulus.

Acknowledgments

We thank William H. Robinson and Henry E. Neuman de Vegvar for discussions regarding array data analysis and Julie Miller, Thomas W. Fleury, and Ryoko Sekine for technical assistance.

Disclosures

The authors have no financial conflict of interest.

References

1. Forbes, S. A., and J. Trowsdale. 1999. The MHC quarterly report. *Immunogenetics* 50: 152–159.
2. Gruen, J. R., and S. M. Weissman. 1997. Evolving views of the major histocompatibility complex. *Blood* 90: 4252–4265.
3. Allcock, R. J., A. M. Martin, and P. Price. 2000. The mouse as a model for the effects of MHC genes on human disease. *Immunol. Today* 21: 328–332.
4. Morahan, G., and L. Morel. 2002. Genetics of autoimmune diseases in humans and in animal models. *Curr. Opin. Immunol.* 14: 803–811.
5. Kotzin, B. L. 1996. Systemic lupus erythematosus. *Cell* 85: 303–306.
6. Wakeland, E. K., K. Liu, R. R. Graham, and T. W. Behrens. 2001. Delineating the genetic basis of systemic lupus erythematosus. *Immunity* 15: 397–408.
7. Gaffney, P. M., W. A. Ortmann, S. A. Selby, K. B. Shark, T. C. Ockenden, K. E. Rohlf, N. L. Walgrave, W. P. Boyum, M. L. Malmgren, M. E. Miller, et al. 2000. Genome screening in human systemic lupus erythematosus. *Am. J. Hum. Genet.* 66: 547–556.
8. Theofilopoulos, A. N., and F. J. Dixon. 1985. Murine models of systemic lupus erythematosus. *Adv. Immunol.* 37: 269–390.
9. Ibnou-Zekri, N., T. J. Vyse, S. J. Rozzo, M. Iwamoto, T. Kobayakawa, B. L. Kotzin, and S. Izui. 1999. MHC-linked control of murine SLE. *Curr. Top. Microbiol. Immunol.* 246: 275–280.
10. Vidal, S., D. H. Kono, and A. N. Theofilopoulos. 1998. Loci predisposing to autoimmunity in MRL-*Fas lpr* and C57BL/6-*Faslpr* mice. *J. Clin. Invest.* 101: 696–702.
11. Jevnikar, A. M., M. J. Grusby, and L. H. Glimcher. 1994. Prevention of nephritis in major histocompatibility complex class II-deficient MRL-*lpr* mice. *J. Exp. Med.* 179: 1137–1143.
12. Andrews, B. S., R. A. Eisenberg, A. N. Theofilopoulos, S. Izui, C. B. Wilson, P. J. McConahey, E. D. Murphy, J. B. Roths, and F. J. Dixon. 1978. Spontaneous murine lupus-like syndromes. *J. Exp. Med.* 148: 1198–1215.
13. Schur, P. H. 1989. Clinical feature of SLE. In *Textbook of Rheumatology.* W. N. Kelly, E. D. Harris, S. Ruddy, and C. B. Sledge, eds. W. B. Saunders, Philadelphia, pp. 1101–1111.
14. Couser, W. G., D. J. Salant, M. P. Madaio, S. Adler, and G. C. Groggel. 1982. Factors influencing glomerular and tubulointerstitial patterns of injury in SLE. *Am. J. Kidney Dis.* 2: 126–134.
15. Glassock, R. J., A. H. Cohen, S. G. Adler, and H. J. Ward. 1991. Secondary glomerular disease. In *The Kidney.* B. M. Brenner and F. C. Rector, eds. W. B. Saunders, Philadelphia, pp. 1280–1288.
16. Winfield, J. B., I. Faiferman, and D. Koffler. 1977. Avidity of anti-DNA antibodies in serum and IgG glomerular eluates from patients with systemic lupus erythematosus. *J. Clin. Invest.* 59: 90–96.
17. Pankewycz, O. G., P. Migliorini, and M. P. Madaio. 1987. Polyreactive autoantibodies are nephritogenic in murine lupus nephritis. *J. Immunol.* 139: 3287–3294.
18. Takahashi, S., M. Nose, J. Sasaki, T. Yamamoto, and M. Kyogoku. 1991. IgG3 production in MRL/*lpr* mice is responsible for development of lupus nephritis. *J. Immunol.* 147: 515–519.
19. Reininger, L., T. Berney, T. Shibata, F. Spertini, R. Merino, and S. Izui. 1990. Cryoglobulinemia induced by a murine IgG3 rheumatoid factor: skin vasculitis and glomerulonephritis arise from distinct pathogenic mechanisms. *Proc. Natl. Acad. Sci. USA* 87: 10038–10042.
20. Izui, S., T. Berney, T. Shibata, and T. Fulpius. 1993. IgG3 cryoglobulins in autoimmune MRL-*lpr* mice. *Ann. Rheum. Dis*. (52 Suppl. 1): S48–S54.
21. Mixter, P. F., J. Q. Russell, F. H. Durie, and R. C. Budd. 1995. Decreased $CD4^-CD8^-TCR\text{-}\alpha\beta^+$ cells in *lpr/lpr* mice lacking β_2-microglobulin. *J. Immunol.* 154: 2063–2074.
22. Robinson, W. H., C. DiGennaro, W. Hueber, B. B. Haab, M. Kamachi, E. J. Dean, S. Fournel, D. Fong, M. C. Genovese, H. E. de Vegvar, et al. 2002. Autoantigen microarrays for multiplex characterization of autoantibody responses. *Nat. Med.* 8: 295–301.
23. Haab, B. B., M. J. Dunham, and P. O. Brown. 2001. Protein microarrays for highly parallel detection and quantitation of specific proteins and antibodies in complex solutions. *Genome Biol.* 2: RESEARCH 4.0001–4.0013.
24. Tusher, V. G., R. Tibshirani, and G. Chu. 2001. Significance analysis of microarrays applied to the ionizing radiation response. *Proc. Natl. Acad. Sci. USA* 98: 5116–5121.
25. Storey, J. D. 2002. A direct approach to false discovery rates. *J. R. Stat. Soc. Ser. B Stat. Methodol.* 64: 479–498.
26. Eisen, M. B., P. T. Spellman, P. O. Brown, and D. Botstein. 1998. Cluster analysis and display of genome-wide expression patterns. *Proc. Natl. Acad. Sci. USA* 95: 14863–14868.
27. Sekine, H., C. M. Reilly, I. D. Molano, G. Garnier, A. Circolo, P. Ruiz, V. M. Holers, S. A. Boackle, and G. S. Gilkeson. 2001. Complement component C3 is not required for full expression of immune complex glomerulonephritis in MRL/*lpr* mice. *J. Immunol.* 166: 6444–6451.
28. Eisenberg, R. A., J. B. Winfield, and P. L. Cohen. 1982. Subclass restriction of anti-Sm antibodies in MRL/*lpr* mice. *J. Immunol.* 129: 2146–2149.
29. Lefkowith, J. B., and G. S. Gilkeson. 1996. Nephritogenic autoantibodies in lupus: current concepts and continuing controversies. *Arthritis Rheum.* 39: 894–903.
30. Sekine, H., H. Watanabe, and G. S. Gilkeson. 2004. Enrichment of antiglomerular antigen antibody-producing cells in the kidneys of MRL/MpJ-Fas^{lpr} mice. *J. Immunol.* 172: 3913–3921.
31. Watanabe, H., G. Garnier, A. Circolo, R. A. Wetsel, P. Ruiz, V. M. Holers, S. A. Boackle, H. R. Colten, and G. S. Gilkeson. 2000. Modulation of renal disease in MRL/*lpr* mice genetically deficient in the alternative complement pathway factor B. *J. Immunol.* 164: 786–794.
32. Robinson, W. H., P. Fontoura, B. J. Lee, H. E. de Vegvar, J. Tom, R. Pedotti, C. D. DiGennaro, D. J. Mitchell, D. Fong, P. P. Ho, et al. 2003. Protein microarrays guide tolerizing DNA vaccine treatment of autoimmune encephalomyelitis. *Nat. Biotechnol.* 21: 1033–1039.
33. Neuman de Vegvar, H. E., R. R. Amara, L. Steinman, P. J. Utz, H. L. Robinson, and W. H. Robinson. 2003. Microarray profiling of antibody responses against simian-human immunodeficiency virus. *J. Virol.* 77: 11125–11138.
34. Hueber, W., B. A. Kidd, B. H. Tomooka, B. J. Lee, B. Bruce, J. F. Fries, G. Sonderstrup, P. Monach, J. W. Drijfhout, W. J. van Venrooij, et al. 2005. Antigen microarray profiling of autoantibodies in rheumatoid arthritis. *Arthritis Rheum.* 52: 2645–2655.
35. Zhen, Q. L., C. Xie, T. Wu, M. Mackay, C. Aranow, C. Putterman, and C. Mohan. 2005. Identification of autoantibody clusters that best predict lupus disease activity using glomerular proteome arrays. *J. Clin. Invest.* 115: 3428–3439.
36. Sharp, G. C., W. S. Irvin, C. M. May, H. R. Holman, F. C. McDuffie, E. V. Hess, and F. R. Schmid. 1976. Association of antibodies to ribonucleoprotein and Sm antigens with mixed connective-tissue disease, systematic lupus erythematosus and other rheumatic diseases. *N. Engl. J. Med.* 18: 1149–1154.
37. Cohen, P. L., E. Creech, D. Nakul-Aquaronne, R. McDaniel, S. Ackler, R. G. Rapoport, E. S. Sobel, and R. A. Eisenberg. 1993. Antigen nonspecific effect of major histocompatibility complex haplotype on autoantibody levels in systemic lupus erythematosus-prone *lpr* mice. *J. Clin. Invest.* 91: 2761–2768.
38. Arnett, F. C. 2000. Genetic studies of human lupus in families. *Intern. Rev. Immunol.* 19: 297–317.
39. Olsen, M. L., F. C. Arnett, and J. D. Reveille. 1993. Contrasting molecular patterns of MHC class II alleles associated with the anti-Sm and anti-RNP precipitin autoantibodies in systemic lupus erythematosus. *Arthritis Rheum.* 36: 94–104.
40. Arnett, F. C. 1997. The genetics of human lupus. In *Dubois' Lupus Erythematosus*, 5th Ed. D. J. Wallace and B. H. Hahn, eds. Williams & Wilkins, Baltimore, pp. 77–117.
41. Merino, R., L. Fossati, M. Lacour, R. Lemoine, M. Higaki, and S. Izui. 1992. H-2-linked control of the *Yaa* gene-induced acceleration of lupus-like autoimmune disease in BXSB mice. *Eur. J. Immunol.* 22: 295–299.
42. Merino, R., M. Iwamoto, M. E. Gershwin, and S. Izui. 1994. The *Yaa* gene abrogates the major histocompatibility complex association of murine lupus in $(NZB \times BXSB)F_1$ hybrid mice. *J. Clin. Invest.* 94: 521–525.
43. Ibnou-Zekri, N., M. Iwamoto, L. Fossati, P. J. McConahey, and S. Izui. 1997. Role of the major histocompatibility complex class II Ea gene in lupus susceptibility in mice. *Proc. Natl. Acad. Sci. USA* 94: 14654–14659.
44. Ibnou-Zekri, N., M. Iwamoto, M. E. Gershwin, and S. Izui. 2000. Protection of murine lupus by the Ead transgene is MHC haplotype-dependent. *J. Immunol.* 164: 505–511.
45. Mathis, D. J., C. Benoist, V. E. Williams II, M. Kanter, and H. O. McDevitt. 1983. Several mechanisms can account for defective Eα gene expression in different mouse haplotypes. *Proc. Natl. Acad. Sci. USA* 80: 273–277.
46. Kong, P. L., T. Zhu, M. P. Madaio, and J. Craft. 2003. Role of the H-2 haplotype in Fas-intact lupus-prone MRL mice. *Arthritis Rheum.* 48: 2992–2995.
47. Chan, O. T., L. G. Hannum, A. M. Haberman, M. P. Madaio, and M. J. Shlomchik. 1999. A novel mouse with B cells but lacking serum antibody reveals an antibody-independent role for B cells in murine lupus. *J. Exp. Med.* 189: 1639–1648.
48. Matthews, V. B., F. T. Christiansen, and P. Price. 2000. A novel locus affecting serum levels of IgG2a maps to the murine H2 region. *Eur. J. Immunogenet.* 27: 135–139.
49. Matthews, V. B., G. Morahan, and P. Price. 2001. A locus affecting immunoglobulin isotype selection (Igis1) maps to the MHC region in C57BL, BALB/c and NOD mice. *Immunol. Cell Biol.* 79: 576–582.
50. Cunningham-Rundles, C., M. Fotino, O. Rosina, and J. B. Peter. 1991. Selective IgA deficiency, IgG subclass deficiency, and the major histocompatibility complex. *Clin. Immunol. Immunopathol.* 61: S61–S69.

51. Matthews, V. B., C. S. Witt, M. A. French, H. K. Machulla, E. G. De la Concha, K. Y. Cheong, P. Vigil, P. N. Hollingsworth, K. J. Warr, F. T. Christiansen, and P. Price. 2002. Central MHC genes affect IgA levels in the human: reciprocal effects in IgA deficiency and IgA nephropathy. *Hum. Immunol.* 63: 424–433.
52. Eisenberg, R. A., S. Y. Craven, R. W. Warren, and P. L. Cohen. 1987. Stochastic control of anti-Sm autoantibodies in MRL/*Mp-lpr/lpr* mice. *J. Clin. Invest.* 80: 691–697.
53. Gyotoku, Y., M. Abdelmoula, F. Spertini, S. Izui, and P. H. Lambert. 1987. Cryoglobulinemia induced by monoclonal immunoglobulin G rheumatoid factors derived from autoimmune MRL/*lpr* mice. *J. Immunol.* 138: 3785–3792.
54. Fulpius, T., F. Spertini, L. Reininger, and S. Izui. 1993. Immunoglobulin heavy chain constant region determines the pathogenicity and the antigen-binding activity of rheumatoid factor. *Proc. Natl. Acad. Sci. USA* 90: 2345–2349.
55. Smoyer, W. E., and P. Mundel. 1998. Regulation of podocyte structure during the development of nephrotic syndrome. *J. Mol. Med.* 76: 172–183.
56. Sinniah, R., and P. H. Feng. 1976. Lupus nephritis: correlation between light, electron microscopic and immunofluorescent findings and renal function. *Clin. Nephrol.* 6: 340–351.
57. Hall-Craggs, M., and E. Ramos. 1981. Transformation of diffuse proliferative glomerulonephritis to membranous nephritis in a patient with SLE. *Nephron* 28: 42–45.
58. Tornroth, T., E. Honkanen, and E. Pettersson. 1987. The evolution of membranous glomerulonephritis reconsidered. *Clin. Nephrol.* 28: 107–117.
59. Ben-Bassat, M., J. Rosenfeld, H. Joshua, B. Hazaz, and V. Gura. 1979. Lupus nephritis: electron-dense and immunofluorescent deposits and their correlation with proteinuria and renal function. *Am. J. Clin. Pathol.* 72: 186–193.
60. Gessner, J. E., H. Heiken, A. Tamm, and R. E. Schmidt. 1998. The IgG Fc receptor family. *Ann. Hematol.* 76: 231–248.
61. Matsumoto, K., N. Watanabe, B. Akikusa, K. Kurasawa, R. Matsumura, Y. Saito, I. Iwamoto, and T. Saito. 2003. Fc receptor-independent development of autoimmune glomerulonephritis in lupus-prone MRL/*lpr* mice. *Arthritis Rheum.* 48: 486–494.
62. Han, Y., T. R. Kozel, M. X. Zhang, R. S. MacGill, M. C. Carroll, and J. E. Cutler. 2001. Complement is essential for protection by an IgM and an IgG3 monoclonal antibody. *J. Immunol.* 167: 1550–1557.